communications biology

Article

https://doi.org/10.1038/s42003-024-06181-x

Leukemia circulation kinetics revealed through blood exchange method

Check for updates

Alex B. Miller[1,2], Felicia H. Rodriguez[2,3], Adam Langenbucher[2,4], Lin Lin[2], Christina Bray[2], Sarah Duquette[2,3], Ye Zhang[2], Dan Goulet[2], Andrew A. Lane[5], David M. Weinstock[5,9], Michael T. Hemann[2,6] ✉ & Scott R. Manalis[2,3,7,8] ✉

Leukemias and their bone marrow microenvironments undergo dynamic changes over the course of disease. However, little is known about the circulation kinetics of leukemia cells, nor the impact of specific factors on the clearance of circulating leukemia cells (CLCs) from the blood. To gain a basic understanding of CLC dynamics over the course of disease progression and therapeutic response, we apply a blood exchange method to mouse models of acute leukemia. We find that CLCs circulate in the blood for 1–2 orders of magnitude longer than solid tumor circulating tumor cells. We further observe that: (i) leukemia presence in the marrow can limit the clearance of CLCs in a model of acute lymphocytic leukemia (ALL), and (ii) CLCs in a model of relapsed acute myeloid leukemia (AML) can clear faster than their untreated counterparts. Our approach can also directly quantify the impact of microenvironmental factors on CLC clearance properties. For example, data from two leukemia models suggest that E-selectin, a vascular adhesion molecule, alters CLC clearance. Our research highlights that clearance rates of CLCs can vary in response to tumor and treatment status and provides a strategy for identifying basic processes and factors that govern the kinetics of circulating cells.

Leukemias are hematopoietic cancers characterized by the transit of malignant cells through the blood[1]. They arise from mutations in cells within specific sites of hematopoietic development, but quickly spread via circulating leukemia cells (CLCs) to sites throughout the body and have heavy involvement of not only hematological organs such as lymph nodes and spleen, but also the liver and central nervous system[2–4]. Several historical studies have examined the clearance rates of solid tumor circulating tumor cells (CTCs) in mice[5–8], which are the metastatic analogs of CLCs in non-hematological tumors[9,10]. However, these studies relied on collecting blood samples from different mice at discrete timepoints, or using continuous detection in small capillaries, which leads to low accuracy measurements due to mouse-to-mouse heterogeneity or under-sampling of events. Our group has developed a system for continuous monitoring of fluorescent CTCs through the carotid artery of mice, allowing for highly accurate measures of real-time CTC concentration[11]. We previously used this system to identify kinetics of solid tumor CTCs in mice, and reported that half-life times across a variety of tumor types range between 1 and 4 minutes[12]. However, the measurement of circulation kinetics of leukemia CLCs and comparison to solid tumor CTCs has not yet been explored. These measurements may help explain fundamental questions related to the biology of leukemias. For example, the higher burden of some leukemias observed in the blood could result from a greater rate of intravasation (i.e., more entry), lower rate of extravasation (i.e., less exit), or both.

In the context of active leukemia, the bone marrow niche undergoes a number of physical and functional changes. Compared to healthy marrow, leukemic marrow commonly exhibits hypercellularity, enhanced extracellular matrix deposition, vascular adhesion protein expression, and vascular permeability[13–17]. However, little is known regarding the circulation

[1]Harvard-MIT Department of Health Sciences and Technology, Institute for Medical Engineering and Science, Massachusetts Institute of Technology, Boston, MA, USA. [2]David H. Koch Institute for Integrative Cancer Research, Massachusetts Institute of Technology, Cambridge, MA, USA. [3]Department of Biological Engineering, Massachusetts Institute of Technology, Cambridge, MA, USA. [4]Department of Computation and Systems Biology, Massachusetts Institute of Technology, Cambridge, MA, USA. [5]Department of Medical Oncology, Dana-Farber Cancer Institute, Harvard Medical School, Boston, MA, USA. [6]Department of Biology, Massachusetts Institute of Technology, Cambridge, MA, USA. [7]Broad Institute of MIT and Harvard, Cambridge, MA, USA. [8]Department of Mechanical Engineering, Massachusetts Institute of Technology, Cambridge, MA, USA. [9]Present address: Merck and Co., Rahway, NJ, USA. ✉e-mail: hemann@mit.edu; srm@mit.edu

properties of leukemia cells or the factors that regulate circulation. Recent studies have suggested that adhesion proteins, including collagen, fibronectin, and selectins, play an important role in developing a protective niche within the bone marrow. For example, integrin β1 adhesion has been shown to induce chemoprotective drug efflux in acute lymphocytic leukemia (ALL), and interfering with this adhesion pathways has been shown to increase chemotherapeutic efficacy[18–21]. Additionally, E-selectin has been shown to play an important role in leukemia development and trafficking. E-selectin is an endothelial surface protein preferentially expressed on the endothelium of the bone marrow. In healthy animals, E-selectin allows for leukocytes to home to the bone marrow by recognizing sialylated carbohydrates expressed on white blood cells. E-selectin can also be upregulated by endothelial cells upon exposure to cytokines such as IL-1 and TNF-α, which allows for the recruitment of leukocytes to sites of inflammation[22]. However, leukemias have been shown to upregulate some of these cytokines to allow for increased expression of E-selectin in the bone marrow, which is believed to benefit the leukemia cells by holding them in their protective niche[1]. E-selectin has also been associated with chemoresistance in leukemia through the activation of pro-survival signaling[23]. In a mouse model of acute myeloid leukemia (AML), leukemia cells with the highest binding affinity to E-selectin showed the highest resistance to chemotherapy[24]. Finally, the interference of E-selectin binding through small molecule inhibition promotes malignant cell egress from the bone marrow into the blood and resensitizes leukemia cells to chemotherapy[24–26]. A small molecule E-selectin inhibitor (uproleselan), in combination with chemotherapy, has completed phase 1 and phase 2 clinical trials in AML, demonstrating safety and early evidence of efficacy, and is being explored in an ongoing pivotal phase 3 trial[25,27].

Additional studies have suggested that chemotherapeutic treatment of leukemias alters their transcriptional and phenotypic states compared to their untreated counterparts, including the upregulation of adhesion molecules[24,28]. Indeed, there is now extensive literature suggesting that elevated cell adhesion can mediate leukemia resistance to chemotherapy[29,30]. However, few studies have explored changes in leukemia cell circulation properties following disease relapse, and there has, consequently, been little functional validation that upregulation of adhesion molecules alters leukemia circulation kinetics.

Here, we address these questions by employing a blood exchange system to quantify and model circulation kinetics of both ALL and AML models. These data reveal that the half-life time of leukemia cells is over 40 times longer than that of solid tumor CTCs. We then vary the donor-recipient pairs to identify factors that govern the circulation. We find that the presence of ALL in the bone marrow at least 8 days post tumor initiation can limit the clearance of cells from the blood and can be reversed by blocking the vascular adhesion protein E-selectin. Finally, we show that CLCs from a relapsed AML model, but not an ALL model, have faster rates of clearance compared to an untreated version of the same model. This enhanced clearance rate is associated with higher expression of E-selectin ligands. Interfering with E-selectin decreases the clearance of relapse cells. Altogether, this platform identifies critical differences in circulation profiles between solid tumor CTCs and CLCs, as well as between untreated and relapsed leukemia, and provides a method for identifying the impact of specific factors, such as adhesion proteins, on CLC clearance in the blood.

Results

Blood exchange for measuring circulation properties of CLCs

To measure the clearance profile of CLCs, we used a modified version of our previously published blood exchange method[11,12]. By connecting the circulation of a fluorescent-leukemia-bearing donor mouse to a non-leukemia-bearing (healthy) recipient mouse, naturally shed fluorescent CLCs were intravenously infused into a recipient animal for 30 minutes to 1 hour (Fig. 1a). After disconnecting the mice, we performed a 3-hour post-blood exchange scan of the recipient mouse using a microfluidic fluorescent-detection platform to obtain real-time concentrations of CLCs in the blood. An exponential decay curve of the fluorescent CLCs was then fit to the plot of CLC concentration over time to estimate the clearance profile of CLCs in circulation. Two key properties of clearance were extracted from the decay profiles: fraction remaining and equilibration time. The fraction remaining describes the relative change in concentration over the course of the 3-hour scan and estimates what fraction of the cells are still in circulation by the end of that time period (whether or not they exited and then reentered circulation), assuming that our continuous detection of fluorescent CLCs in the carotid artery is representative of the overall CLC concentration in the mouse's blood. It can be calculated by comparing the CLC concentration at the beginning and end of the post-blood exchange scan using the following equation:

$$\textit{Fraction remaining} = \frac{\textit{Concentration of CLCs at the end of post blood exchange scan}}{\textit{Concentration of CLCs at the start of post blood exchange scan}} \quad (1)$$

The second parameter used to characterize the decay profile was the equilibration time. This parameter is similar to a half-life time and describes how long it takes for the concentration in the blood to reach a steady state. Since not all of the curves decay to zero, it was important to add a constant to the equation, such that there was a decay to constant, rather than a decay to zero (a decay to zero describes a half-life measurement). A best fit curve was applied to the decay data, with inputs of concentration and time in minutes, using the following equation:

$$Concentration = a * e^{time/k} + c \quad (2)$$

where k is the equilibration time in minutes. The parameters a, k, and c were swept over positive values to find the best fit and identify the estimated equilibration time.

We started by testing two fluorescent syngeneic models of leukemia to study circulation kinetics, a BCR-ABL driven B cell ALL model and an MLL-AF9 driven AML model[31–36], each paired with healthy recipients. In these experiments, the calculated constant *c* in the exponential decay equation was found to be near 0, so the equilibration times in these experiments are equivalent to the true half-lives of the CLCs in circulation. Although the circulating concentration of CLCs varied by at least 1000-fold over the 3-week time course of disease (Supplemental Fig. 1a), we observed no significant correlation between days post leukemia initiation and either half-life or fraction remaining (Supplemental Fig. 1b, c), suggesting that the early and later stage CLCs have similar circulation properties in both models.

In a previous study we measured the half-life times of CTCs from three solid tumor models: small cell lung cancer (SCLC), pancreatic ductal adenocarcinoma (PDAC) and non-small cell lung cancer (NSCLC)[12]. Since the solid tumor half-life estimates were also performed through blood exchange with healthy recipient mice, we could compare the half-life times in circulation of the solid tumor CTCs to the CLCs from the leukemia models. Interestingly, we found the half-life times of CLCs to be approximately 200 minutes, compared to between 1 and 5 minutes for the solid tumor models (Fig. 1b). This finding demonstrates that, among the models we tested, solid tumor CTCs have markedly faster clearance in the blood compared to CLCs.

Impact of bone marrow cellularity on clearance of CLCs

A long-standing question in both the leukemia and transplantation fields is whether bone marrow occupancy impacts the dissemination of cells introduced into the circulation[37]. To assess whether the presence of leukemia in the bone marrow can impact the clearance rates of CLCs, we varied the leukemia status of recipient animals in our blood exchange clearance experiments (Fig. 2a). We used a non-fluorescent (RFP-) version of the same BCR-ABL driven ALL leukemia tested previously. We started by comparing clearance rates when RFP + ALL donor mice were connected to healthy recipient mice or to recipients bearing active RFP- ALL with 30-90% leukemia burden in the marrow. We found a striking difference in the clearance

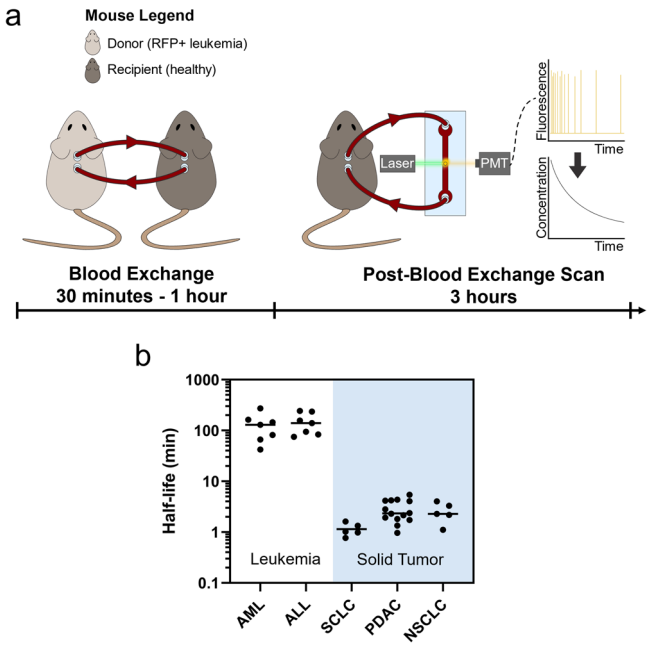

Fig. 1 | Blood exchange identifies differences in clearance kinetics of circulating tumor cells between leukemia and solid tumor models. a Overview schematic of blood exchange setup. A donor and recipient mouse have their circulation connected for 30 minutes to 1 hour. Following this blood exchange period, the mice are disconnected and the circulation from the recipient mouse is monitored for three hours. The blood passes through a laser on a microfluidic chip, and emitted light from fluorescent CLCs is detected by a photomultiplier tube (PMT). The raw data from the PMT is then processed to identify the concentration of CLCs, and the decay profile is used to extract circulation parameters. **b** Half-life times of circulating leukemia cells (AML and ALL) is several orders of magnitude higher than historical measures of various solid tumor circulating tumor cells[12]. SCLC small-cell lung cancer, PDAC pancreatic ductal adenocarcinoma, NSCLC non-small-cell lung cancer. Each dot represents an independent donor-recipient mouse pair.

profiles (Fig. 2b, c: Healthy Mouse and Leukemia). While clearance of RFP + ALL CLCs followed a steady decrease over the 3-hour post-blood exchange scan when infused into healthy recipients, there was an 84% increase in the fraction remaining term (Eq. 1) with RFP- ALL-bearing recipients. However, no correlation was observed between days post tumor initiation (a proxy for engraftment) and clearance kinetics over the engraftment range of approximately 30–90% (Supplemental Fig. 1a–c).

It is worth noting that young adult mouse bone marrow is highly cellular (typically >95%) so the longer equilibration time in leukemic recipients is less likely to simply result from less availability of space for engraftment and more likely result from remodeling induced by the engrafted leukemia. To test this hypothesis, we treated mice engrafted with RFP- ALL with a one-time dose of cyclophosphamide (CTX) and performed blood exchange 2-5 days post treatment. This dose resulted in a decrease in percentage of leukemia cells to below 5% through day 5 post treatment, and approximately a 3-week survival extension (see Methods). In the CTX-treated mice, the clearance profile and fraction remaining returned to that of the healthy mice (Fig. 2b, c; Supplemental Fig. 2a: Treated leukemia). The data showed an approximately 2-fold increase in fraction remaining in the diseased (RFP-) recipients compared with healthy mouse (HM) recipients, about 0.6 compared to 0.3. This phenotype was fully reversed with CTX treatment, where the clearance of CLCs in recipient mice returned to a fraction remaining of approximately 0.3. These preliminary findings suggest that the presence of an existing leukemia burden actively reduces the clearance of CLCs in a manner that rapidly reverses with treatment. Of note, because the changes were reversed within several days of CTX treatment, it is unlikely that such changes are due to vascular remodeling since these processes can take up to three weeks to be observed[38].

As a next step, we further addressed whether the reduced bone marrow cellularity from treatment directly promotes CLC clearance. To that end, we compared the clearance rates of RFP + ALL CLCs in healthy recipients that had been treated either with CTX or irradiation. First, we confirmed that both chemotherapy treatment and irradiation induced hypocellularity in the bone marrow of healthy mice (Supplemental Fig. 3a), and quantification revealed a drop in total number of cells in the marrow of approximately 65-75% (Supplemental Fig. 3b). We then performed blood exchange experiments using ALL-bearing donor mice and monitored the decay in the post-blood exchange scan (Supplemental Fig. 3c). While there were small changes in the clearance profiles, there were no significant decreases in the fraction remaining at the end of the post-blood exchange scan in either the irradiated or chemotherapy-treated recipients (Supplemental Fig. 3d). Our experiments demonstrate that decreasing marrow cellularity alone through myeloablation is insufficient to alter circulation kinetics. This suggests that the decreased clearance observed in diseased animals that was reversed upon chemotherapy treatment is also not solely due to changes in marrow cellularity. Instead, we hypothesize that molecular changes associated with the presence of disease drive these phenotypes and revert once a sufficient fraction of the disease is cleared. These preliminary data suggest that engraftment kinetics may be affected by disease state more than bone marrow cellularity. This is noteworthy considering varied clinical approaches to recipient conditioning and bone marrow clearance prior to hematopoietic stem cell or T cell transplantation that could be studied using this approach[39,40].

Impact of bone marrow adhesion mediators on clearance of CLCs

To gauge the ability of this approach to monitor leukemia cell clearance kinetics following perturbations to the leukemia microenvironment, we focused on E-selectin, an endothelial surface protein. E-selectin attaches to several glycans and glycoproteins by binding to sialylated carbohydrates[41], is important in leukocyte recruiting, and is upregulated in response to inflammatory cytokines, including TNF-α (tumor necrosis factor α) and IL-2 (interleukin 2)[1]. Additionally, a previous study showed that the inhibition of E-selectin led to an increase in the circulating number of CLCs in a model of AML[24]. To determine the potential relevance of E-selectin on our ALL model, we monitored E-selectin levels over the course of leukemia treatment. We also allowed the treated mice to relapse (>50% in the bone marrow at 2.5 weeks post treatment), and measured E-selectin expression at relapse. Notably, we found an increase in the percent of E-selectin positive bone marrow endothelial cells (BMECs) from about 5% for healthy and acutely treated mice to around 15% in diseased and relapse mice (Fig. 2d). This finding is similar to what we observed in the blood exchange experiments with diseased and treated mice, where a shift in leukemia clearance kinetics with a diseased recipient was reversed through treatment. Notably, a different endothelial binding protein, VCAM1 (vascular cell adhesion molecule 1), which binds to the integrin VLA4 (very late antigen 4 α4β1) and has been implicated in regulating ALL chemotherapy resistance[18,20], was found to not correlate with disease state (Supplemental Fig. 4). The observed increase of E-selectin on BMECs in the context of disease, and subsequent decrease upon treatment has not previously been explored in ALL but matches previously reported findings of acutely treated AML. Historical data suggests AML cells create inflammatory signaling that upregulates E-selectin expression on BMECs[24], though no assessment of E-selectin expression on BMECs at late relapse has previously been reported. This association between leukemia status and E-selectin expression was also observed on BMECs from the AML model (Supplemental Figure 5).

Since E-selectin expression on BMECs changed over the course of disease and treatment, we decided to test whether inhibiting E-selectin using blocking antibodies would reverse the shift in clearance kinetics observed from blood exchange experiments. We used RFP + ALL-bearing mice as the donors of blood exchange with RFP- ALL-bearing recipients treated with 100 μg of α-E-selectin antibody or vehicle control 20 min before the start of blood exchange. Consistent with the previous study in AML[24], we

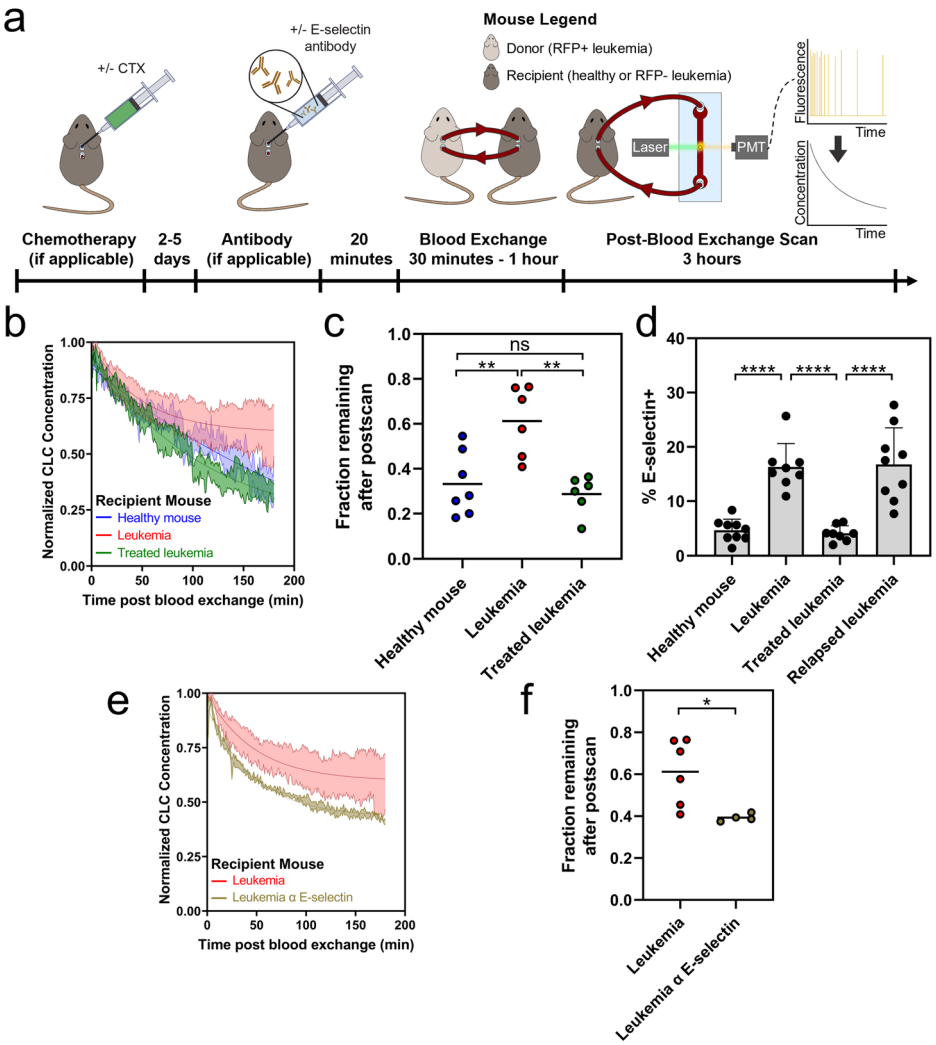

Fig. 2 | Bone marrow microenvironment can impact clearance of CLCs. a Overview of experimental plan. Some mice (**e**, **f**) are dosed with E-selectin antibody prior to blood exchange and postscan. **b** Decay profiles of RFP+ CLCs in recipients with varied tumor status. **c** Decreased clearance of CLCs in recipient mice with active disease as measured by an increase in fraction of CLCs remaining in circulation (Tukey multiple comparisons $^{**}p < 0.01$). **d** E-selectin expression on BMECs increases in diseased context (bars represent mean ±standard deviation; Tukey multiple comparisons $^{****}p < 0.0001$). **e** Decay profiles of RFP+ CLCs in tumor bearing recipient mice with or without E-selectin antibody treatment. **f** Dosing recipient mice with E-selectin antibody allows for increased clearance of CLCs in diseased recipients as measured by decrease in fraction remaining (two-tailed t test $p = 0.0254$). For decay profiles (**b**, **e**), shaded regions are represented by mean +/- standard error, and lines represent the best fit decay curve. For fraction remaining analysis (**c**, **f**), each dot represents an independent donor-recipient mouse pair.

found that dosing with E-selectin antibody intravenously was able to increase the circulating concentration of ALL CLCs within 20 minutes (Supplemental Figure 6). The decay profile of RFP- mice dosed with E-selectin antibody showed a distinct shift from the non-dosed RFP- recipient mice (Fig. 2e), and the fraction remaining at the end of post-blood exchange scan was found to be significantly lower ($p = 0.0254$) in diseased mice treated with E-selectin antibody, while the equilibration rate was unchanged (Fig. 2f; Supplemental Fig. 2b). These results show that disrupting E-selectin binding increases the number of ALL CLCs, at least in part, by reducing clearance. Importantly, this data demonstrates that the blocking of E-selectin, and subsequent impact on the ability of leukemia cells to interchange between blood and marrow, alters the clearance rates of newly added donor CLCs as compared to an untreated diseased animal. Future work will be necessary to determine whether blocking E-selectin is sufficient to return the clearance profile to that of a healthy mouse. Additionally, these data suggest that our approach can provide high resolution measurements of leukemia kinetics following perturbations that potentially impact leukemia cell retention in bone marrow or other sites of persistent disease.

Impact of relapse status on clearance of CLCs

To address whether cellular changes after chemotherapy can alter the circulation profile of CLCs, we used treated and untreated leukemia-bearing animals as donors in our blood exchange pairs. This allowed for the study of how untreated or relapsed CLCs clear in healthy recipient mice and served as a method for decoupling changes imparted from the bone marrow microenvironment with those imparted from the leukemia cells themselves. We performed these experiments using both the ALL and AML models. For these experiments, relapse was defined by leukemia regrowth to at least 50% in the marrow following treatment and nadir. In our ALL model, we saw similar clearance kinetics in the recipient healthy mice with either untreated or relapse donor CLCs, with no change in the equilibration time or fraction remaining (Fig. 3a, b, Supplemental Figure 7a). However, in the relapsed AML model, CLCs had a more rapid initial clearance (Fig. 3c, d, Supplemental Fig. 7b). Quantitatively, this was reflected in the equilibration times, where relapse CLCs had a significantly faster equilibration time than the untreated CLCs, with over 100 minutes for untreated CLCs compared to around 20 minutes for the relapse CLCs.

We next wondered if changes in E-selectin could underlie the altered CLC kinetics between untreated and relapsed AML. Because E-selectin, found on endothelial cells, binds to sialyl groups of glycans and glycoproteins, there is no single antibody to effectively assess the ability of leukemia cells to bind E-selectin[42]. As such, we tested E-selectin binding capacity by incubating the leukemia cells with a fluorescently conjugated E-selectin protein (using a chimera of recombinant mouse E-selectin and human IgG with a fluorescent α-human IgG antibody) (Fig. 3e). Using flow cytometry, we compared the capacity to bind E-selectin between untreated and relapsed disease in both the blood and bone marrow (Fig. 3f). The binding capacity in the AML model for both untreated and relapse states was markedly higher than in the ALL model, and there was a statistically significant increase in the AML model between E-selectin binding of untreated and relapse disease that was not seen in the ALL model. Integrin β1, which has been suggested to

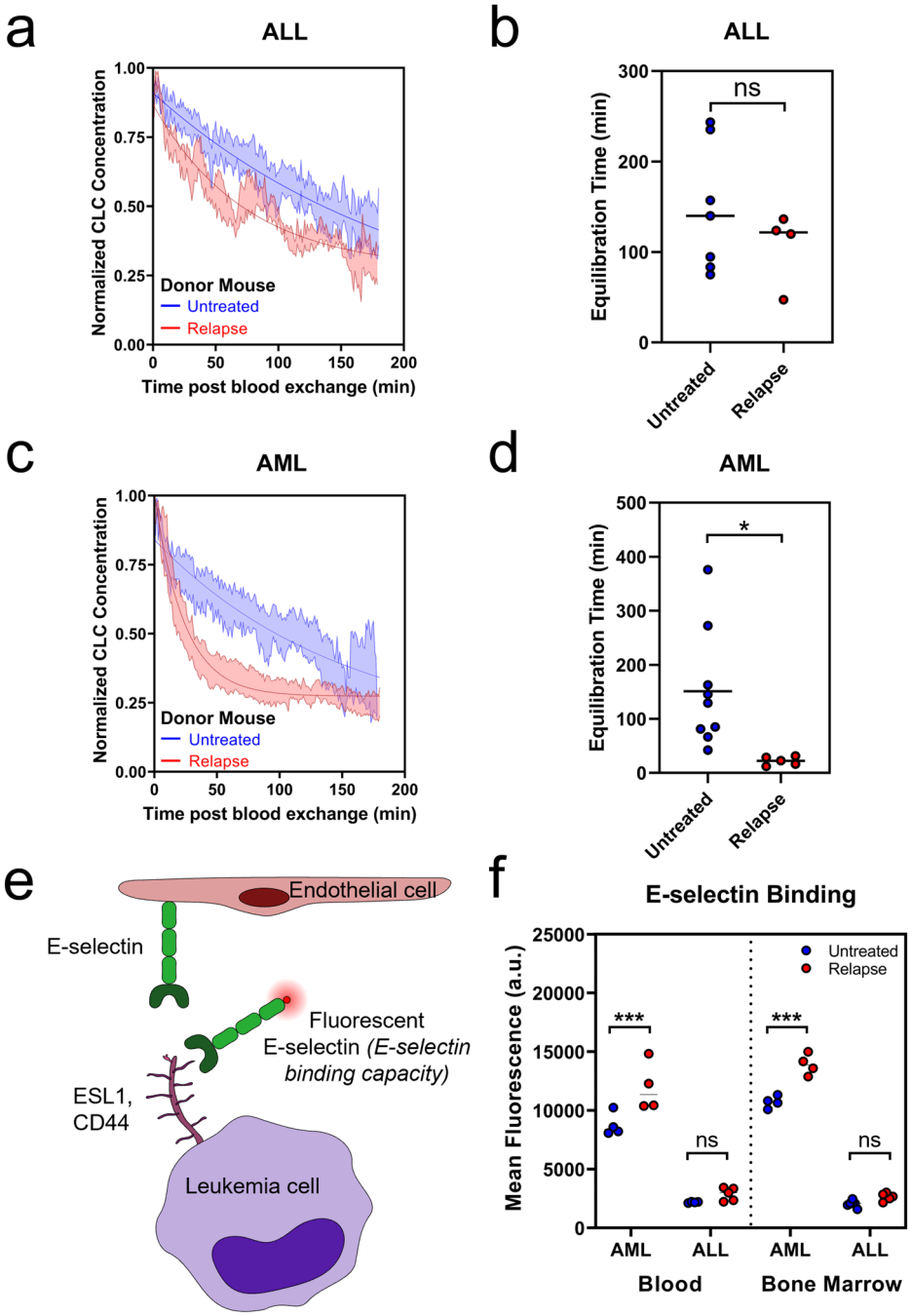

Fig. 3 | Blood exchange identifies differences in clearance kinetics in healthy mice with either untreated or relapse donors. a Decay profiles of untreated and relapse ALL CLCs in healthy recipient mice. **b** Relapse and untreated ALL CLCs have similar kinetics as measured by equilibration time (two-tailed t test p = 0.3257). **c** Decay profiles of untreated and relapse AML CLCs in healthy recipient mice. **d** Equilibration time of relapse AML CLCs significantly faster than untreated (two-tailed t test $p = 0.0230$). **e** Schematic of E-selectin adhesion to endothelial cells and E-selectin binding assay using fluorescent E-selectin. **f** E-selectin binding capacity increases in blood and marrow at relapse in AML and ALL (Tukey multiple comparisons: $^{***}p < 0.001$, ns $p > 0.5$). For decay profiles (**a**, **c**), shaded regions are represented by mean +/− standard error, and lines represent the best fit decay curve. For equilibration time analysis (**b**, **d**), each dot represents an independent donor-recipient mouse pair.

contribute to chemoprotective niche, showed mostly nonsignificant differences (Supplemental Fig. 8). Our findings suggest that the lack of significant increase in the ALL model does not lead to changes in the clearance rates, while the dramatic and statistically significant increase in E-selectin binding in the AML model at relapse may play a role in altering the rate of clearance of relapse CLCs compared to untreated.

The binding capacity of E-selectin and expression of integrin β1 increased acutely post chemotherapy in the bone marrow in both models and remained elevated compared to pre-treatment at relapse (Supplemental Fig. 9). While other studies have similarly shown increases in adhesion expression directly following treatment[24], there has previously been little evidence of whether that expression remains increased at relapse.

We have previously shown that buoyant mass can be a proxy for passage time through a channel[43]. Using a suspended microchannel resonator to measure the buoyant mass of single cells[44–46], we found that there were no significant differences between untreated and relapsed disease for either model in either blood or bone marrow (Supplemental Fig. 10). This suggests that difference in size does not explain the change in circulation that was observed.

Since E-selectin inhibition on endothelial cells was sufficient to alter clearance kinetics in a diseased ALL mouse (as described in Fig. 2), we wanted to explore whether interfering with E-selectin binding of leukemia cells could affect the observed changes associated with treatment in a different disease model. To that end, we dosed relapsed AML mice with recombinant mouse E-selectin 20 minutes prior to blood exchange with a healthy recipient, in order to occupy glycoproteins on the leukemia cell surface (Fig. 4a). We found that mice engrafted with relapsed AML dosed with recombinant E-selectin showed a significantly longer equilibration time and higher fraction remaining in circulation compared to non-treated relapse mice (Fig. 4b–d). These results suggest that the increase in E-selectin

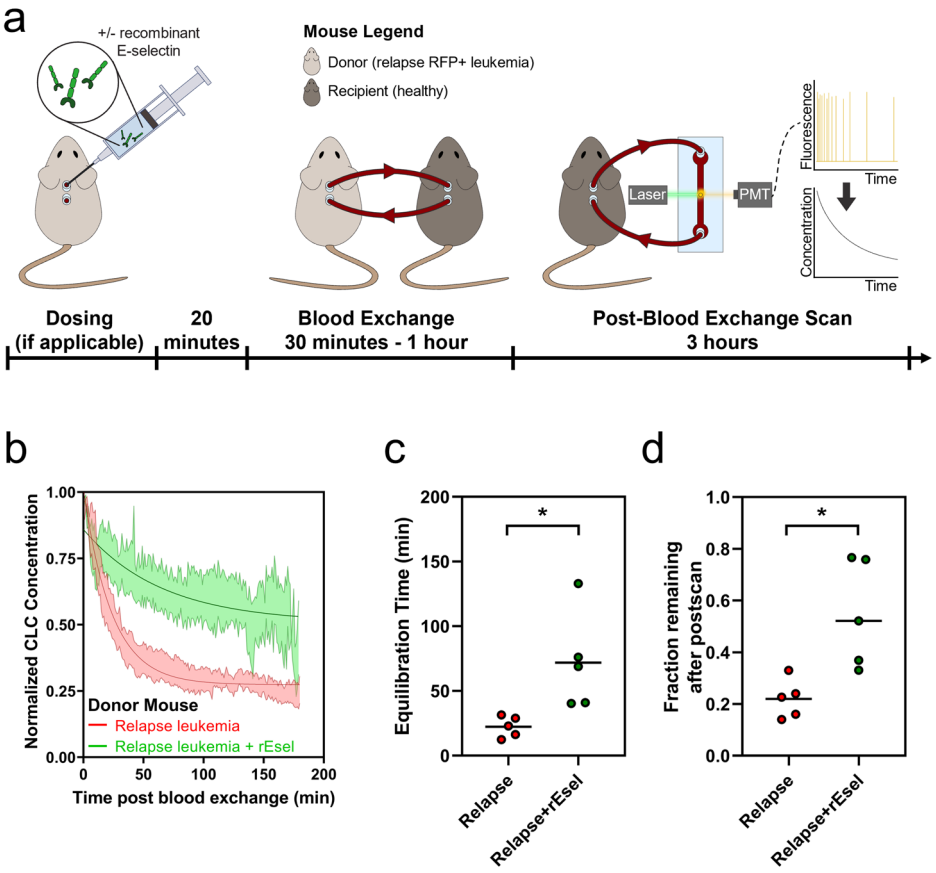

Fig. 4 | Interfering with E-selectin binding decreases clearance of relapse AML CLCs. **a** Overview of experiment. Recombinant E-selectin is added to the relapse donor mouse prior to blood exchange with healthy recipient. **b** Decay profiles of relapse CLCs with or without recombinant E-selectin (rEsel) treatment in healthy recipient mice. **c**, **d** CLCs from relapse mice treated with recombinant E-selectin showed increase in both equilibration time (**c**, two-tailed t test $p = 0.021$) and fraction remaining (**d**, two tailed t-test $p = 0.010$). For decay profiles (**b**), shaded regions are represented by mean±standard error, and lines represent the best fit decay curve. Each dot represents an independent donor-recipient mouse pair.

binding molecules on AML relapse cells increases the ability of the relapse cells to exit circulation faster and demonstrates that inhibiting E-selectin binding can prevent CLCs from rapidly leaving circulation.

Discussion

The data presented here highlight the capability of the blood exchange system to quantify the impact of biological processes and specific factors on the clearance rate of circulating cells. By manipulating donor and recipient mice, we can observe how changes to either circulating or non-circulating factors can directly impact the clearance of CLCs. We demonstrate that changes in the bone marrow, such as the presence of significant leukemia engraftment, as well as treatment status of disease, can alter the clearance profile of CLCs. Our data also suggests that the adhesion molecule E-selectin plays an important role in modulating the clearance rates of CLCs. E-selectin has been explored as a potential therapeutic target for concurrent chemotherapy in AML[25], and the data we have shown here supports this and suggests that other types of leukemia, such as ALL, may also benefit from E-selectin based therapies.

Two core findings of this work are that the circulation time of leukemias may be substantially longer than that found in circulating solid tumor cells and that this circulation time is impacted by the presence of existing disease at sites of leukemia dissemination. While it is perhaps intuitive that blood cancers would have greater propensity to persist in the blood compared to solid tumors, this work highlights that not all disseminating malignancies have acquired similar persistence characteristics. Additionally, this work shows that leukemia cells do not persist for indefinite periods in circulation and that the circulating pool is continually fed from extravascular sites. Thus, this kind of blood exchange system can yield fundamental insight into the dissemination of hematopoietic disease.

That the presence of a significant existing disease burden impacts tumor circulation kinetics is perhaps also not surprising. However, these data have important implications. First, it suggests that dissemination of mutant clones within a leukemia may be impaired in the presence of substantial disease, and that broad dissemination of mutant clones may be facilitated by the ablation of bulk disease. Second, our data shows that eradication of tumor burden is not the same as eradication of normal bone marrow resident cells in promoting tumor clearance and engraftment. How conditioning agents used to prepare patients for stem cell transplantation or adoptive cell therapy impact donor cell engraftment is a fundamental question—one that may be uniquely informed using this type of blood exchange approach.

Our studies also demonstrate that leukemias may experience profound changes in circulation profiles after treatment. While the idea that leukemia adhesion can mediate drug resistance is well-established, the notion that changes in cell adhesiveness and circulation kinetics can stably persist in relapsed tumor cell populations is less appreciated. Indeed, it is logical and concordant with our findings that relapsed tumor cells may survive both initial and subsequent therapies due to their greater propensity to avoid circulation and reside in extravascular sites.

Finally, our findings emphasize a role for adhesion proteins as mediators of therapeutic resistance and potential targets. Due to the discontinuous basement membrane in the sinusoidal capillaries of the bone marrow[47,48], E-selectin expressed on BMECs is directly exposed to both the blood and marrow space[49–52]. Our findings suggest that in the setting of leukemia, high levels of E-selectin on BMECs bind leukemia cells both along the vascular walls and in the marrow, creating a static environment with minimal turn-over between the blood and bone marrow compartments, thereby inhibiting leukemia cells from exiting circulation, as seen by a lack of clearance of the fluorescent donor CLCs. By blocking E-selectin in this environment, leukemia cells in the bone marrow can be released and more freely interchange between tumor compartments of the blood and bone marrow. This hypothesis is consistent with our observation that infused fluorescent CLCs can clear more rapidly in tumor-bearing recipients after treatment with an E-selectin antibody. Given recent results that uprolesolan,

a small molecule E-selectin inhibitor, can increase the potency of chemotherapy in AML[24,25], a central question is whether its efficacy is predominately achieved through local interactions in the marrow, or due to alterations in CLC dynamics. Our system is well-positioned to address this type of question and better understand how novel drugs can impact the circulation kinetics of CLCs, which may change the interpretation of how blood burden in the patient relates to therapy efficacy.

Our study has multiple limitations, including a lack of validation in other mouse models, such as patient-derived xenograft (PDX) models, as well as a lack of genetic perturbations, such as knock-out models of adhesion proteins. However, the goal of this study was to validate the use of this technology to investigate biological questions. Future studies will be needed to explore whether these findings are generalizable across models and identify the mechanism by which specific factors can contribute to alterations in circulation properties of CLCs. Also, the leukemia models studied here are different than the genetically inducible models used in our historical studies to assess solid tumor CTC circulation properties. Future work will be necessary for determining the degree to which the type of model (e.g., syngeneic, PDX, autochthonous) and method of implantation (e.g., intravenous, intraosseous, intrasplenic) impacts the clearance rates of circulating cells. In addition, further studies in immunocompromised mice with human tumors could shed important light on differences between human and mouse leukemias, but several confounding factors, including the xenogeneic interactions with mouse BMECs and the role of the adaptive immune system will need to be considered. Additionally, although we show that treatment with recombinant E-selectin influences the clearance rate of CLCs, we did not perform an in vitro quantification of the reduction in adherence to endothelial cells associated with binding to recombinant E-selectin. Future studies will be needed to assess how the degree of surface protein inhibition impacts the circulation dynamics of CLCs. Another limitation of our study is the focus primarily on the role of E-selectin in regulating CLC clearance rates, when there is a wide array of binding molecules that could impact the circulation of CLCs. Future studies will be necessary to explore additional proteins, including CAMs, cadherins, and integrins, to assess the role they play in CLC trafficking.

Because our system can decouple the influence of circulating and non-circulating factors, we envision that this blood exchange system can be broadly applied across different cancer types to understand the clearance rates of circulating cells and properties that govern cell clearance, from homing and adhesion factors to mechanisms of drug resistance.

Methods

Blood exchange system

The platform used involves the connection of two Mouse CTC Sorter systems[11,12]. Each system consists of a microfluidic device, a laser based optical detection system, and a computer controller. The PDMS microfluidic chip is a 100 μm wide × 45 μm tall channel of 1 cm in length, with a single inlet and a single outlet bonded to a glass slide. The optical detection system consists of a 532 nm laser that is split into two using polarizing beam splitters and is focused into lines on the microfluidic channel using a cylindrical lens. Emitted light passes through the dichroic and is detected by a photomultiplier tube (PMT). The computer controller records the PMT signal and identifies the presence of fluorescent CLCs by their signature double-peak as they pass through the two laser lines. The computer also controls the peristaltic pump which pushes blood through the connective tubing and microfluidic chip at a set rate of 60 μL/min, and the two cameras which observe two regions of the channel to monitor the system.

Model fitting

To identify the concentration of CLCs in the blood, the raw data from the PMT is fed into a MatLab program to identify the peak signatures, and the Eq. 1 & 2 described in the Results section are used to identify the circulation parameters. For Eq. 2, while the value of k is the variable of interest in the equation, the variables a and c are scaling factors used solely to find the best fit for k. The variable c describes the steady state level of circulation in the mice but is much less robust of a measurement than the fraction remaining value. Especially when there is a high concentration in the blood at the end of blood exchange, small changes in measurements in the last few minutes can drastically impact the best-fit c value, with relatively little impact on the k equilibration rate. Similarly, the variable a describes the amplitude from the estimated c to the starting concentration, and thus can also fluctuate with small changes in measurements. As such, the scaling factors a and c are not used for downstream analysis.

Mice

We have complied with all relevant ethical regulations for animal use. All animal procedures were approved by the Massachusetts Institute of Technology Committee on Animal Care (CAC), Division of Comparative Medicine (DCM). Animals were housed on hardwood chip bedding, with a 12/12 h light-dark cycle at a temperature of 70 °F + /− 2 and humidity of 30–70%. All mice used for these studies were C57BL/6 mice procured from Jackson Laboratories.

Because the cancer cell lines used were derived from male mice, all mice in these studies were male. Tumors were initiated when the mice were aged 12–16 weeks. Cells were thawed 1–3 days prior to tumor initiation and passaged daily. On the day of tumor initiation, cells were resuspended in sterile PBS and 500k cells in 100uL were injected via tail vein into each mouse. For the AML model, 1 × 5 Gy of radiation was dosed 24 h before injection of tumor cells to allow for tumor engraftment.

To access the circulation for blood exchange experiments, surgical cannulation was performed. Catheters (Instech: C20PU-MJV1458 and C10PU-MCA1459) were placed into the carotid artery and jugular vein of the mice and were externalized through a vascular access button (Instech: VABM2JB/25R25). Catheters were flushed every 3–4 days with saline before filling with a heparinized locking solution (SAI HGS-10-C). Blood exchanges for untreated mice were performed 6-19 days post tumor initiation.

Each blood exchange is performed with a new donor and recipient mouse.

Drug testing

For the ALL model, a single 50 mg/kg dose of the chemotherapy cyclophosphamide (CTX) was given intraperitoneally (IP) 8 days after tumor initiation of 500k cells via tail vein injection. We found that the CTX treated mice had a 2–3-week life extension compared to the untreated animals (Supplemental Figure 11a). For the AML model, we used a 5 + 3 treatment of cytarabine (araC) and doxorubicin (dox). For 5 days, beginning 8 days post tumor initiation of 500k AML cells, the mice were dosed IP with 20 mg/kg araC. And on the first three of those days (days 8–10 post tumor initiation), mice were given a concurrent dose of 2 mg/kg dox. The 5 + 3 araC/dox treatment provided roughly one week life extension (Supplemental Fig. 11b).

Blood exchange with relapse AML mice was performed 9–16 days post final day of treatment, and blood exchange with relapse ALL mice was performed 13–16 days post treatment.

Flow cytometry

Bone marrow cells were isolated through manual grinding of left and right femurs with mortar and pestle, and red blood cells removed through ACK lysis buffer before 10 minutes FcX blocking BioLegend 101320) and 20 minutes of staining at 4 °C. Blood samples were collected from terminal cardiac puncture, and red blood cells were removed with two rounds of ACK lysis buffer before 10 min FcX blocking and 20 min of staining at 4 °C. Flow cytometry was performed on a BD LSR HTS-2 analyzer. The gating strategy used to identify the fraction of BMECs expressing adhesion proteins is shown in Supplemental Fig. 12. After selecting for single cells through forward and side scatter, endothelial cells were selected as DAPI- (live), CD31+ (endothelial marker [BioLegend: 102410]), and CD45- (white blood cell marker [BioLegend: 103108]). A cutoff on the endothelial cells in the channel of the adhesion molecule antibody (E-selectin [Santa Cruz

Biotechnology: sc-59766 PE] and VCAM1 [Life Technologies: 11-1061-82 FITC]) was used to identify high expressing cells within the BMECs. Because of the low abundance of endothelial cells in the marrow <1%, at least 1 million cells were analyzed per mouse bone marrow sample. To identify the expression of adhesion markers on the leukemia cells, the following strategy was used. To assess for E-selectin binding potential, a recombinant E-selectin human IgG chimera [BioLegend: 755504] was conjugated to fluorescent α-Human IgG [Life Technologies: A10631] for 30 min at room temperature prior to staining[24]. The presence of integrin was determined with an integrin β1 antibody [Life Technologies: 11-0291-82]. After selecting for single cells through forward and side scatter, tumor cells were selected as DAPI- (live), CD45+ (white blood cell marker [BioLegend: 103114]), PE+ (constitutively expressed RFP). Average expression in the channel of the adhesion molecule (E-selectin binding or integrin β1) was then used to assess binding potential.

E-selectin interference

To interfere with BMEC expression of E-selectin, 100 μg (100 μL) of mouse E-selectin antibody (BioLegend: 148803) was injected retro-orbitally 20 min prior to blood exchange in the recipient mouse. To interfere with the expression of E-selectin binding molecules on tumor cells, 20 μg (100 μL) of recombinant mouse E-selectin (BioLegend: 755504) was injected retro-orbitally 20 min prior to blood exchange.

Histology

Femurs were isolated and fixed in formalin for 24 h before being washed and stored in 70% ethanol. Samples were prepared in paraffin wax and sliced into 5 μm sections before hematoxylin and eosin staining. Slides were analyzed on a Nikon A1R confocal microscope.

Statistics and reproducibility

Each blood exchange replicate represents a separate pair of mice. Statistics are performed as described in the text (Tukey multiple comparison or two-tailed T tests where appropriate). Individual datapoints are shown in graphs to identify the number of independent replicates per experiment. At least 2 separate cohorts of mice were used for all blood exchange studies.

Reporting summary

Further information on research design is available in the Nature Portfolio Reporting Summary linked to this article.

Data availability

The data behind the graphs in this study can be found in the supplemental data file. Any additional data is available from the corresponding authors upon reasonable request.

Received: 13 September 2023; Accepted: 10 April 2024;
Published online: 20 April 2024

References

1. Whiteley, A. E., Price, T. T., Cantelli, G. & Sipkins, D. A. Leukaemia: a model metastatic disease. *Nat. Rev. Cancer* **21**, 461 (2021).
2. Mathews, E., Laurie, T., O'Riordan, K. & Nabhan, C. Liver involvement with acute myeloid leukemia. *Case Rep. Gastroenterol.* **2**, 121 (2008).
3. Doolittle, N. D. Brain metastases in hematologic malignancies. *Cancer Treat. Res* **136**, 169–183 (2007).
4. Bross, I. D. J., Viadana, E. & Pickren, J. W. The metastatic spread of myeloma and leukemias in men. *Virchows Arch. A Pathol. Anat. Histol.* **365**, 91–101 (1975).
5. Madden, R. E. & Malmgren, R. A. Quantitative Studies on Circulating Cancer Cells in the Mouse | Cancer Research | American Association for Cancer Research. *Cancer Res.* **22**, 62–66 https://aacrjournals.org/cancerres/article/22/1_Part_1/62/474851/Quantitative-Studies-on-Circulating-Cancer-Cells (1962).
6. Fidler, I. J. Metastasis: quantitative analysis of distribution and fate of tumor emboli labeled with 125I-5-Iodo-2′ -deoxyuridine. *JNCI: J. Natl Cancer Inst.* **45**, 773–782 (1970).
7. Aceto, N., Toner, M., Maheswaran, S. & Haber, D. A. En route to metastasis: circulating tumor cell clusters and epithelial-to-mesenchymal transition. *Trends Cancer* **1**, 44–52 (2015).
8. Meng, S. et al. Circulating tumor cells in patients with breast cancer dormancy. *Clin. Cancer Res* **10**, 8152–8162 (2004).
9. Massagué, J. & Obenauf, A. C. Metastatic colonization by circulating tumour cells. *Nature* **529**, 298–309 (2016).
10. Morgan-Parkes, J. H. Metastases: mechanisms, pathways, and cascades. *Adv. Clin. Med.* **164**, 1075–1082 (1995).
11. Hamza, B. et al. Optofluidic real-time cell sorter for longitudinal CTC studies in mouse models of cancer. *Proc. Natl Acad. Sci. USA* **116**, 2232–2236 (2019).
12. Hamza, B. et al. Measuring kinetics and metastatic propensity of CTCs by blood exchange between mice. *Nat. Commun.* **12**, 1–11 (2021).
13. Chen, Y. et al. Acute myeloid leukemia–induced remodeling of the human bone marrow niche predicts clinical outcome. *Blood Adv.* **4**, 5257–5268 (2020).
14. Kim, J. A. et al. Microenvironmental remodeling as a parameter and prognostic factor of heterogeneous leukemogenesis in acute myelogenous leukemia. *Cancer Res* **75**, 2222–2231 (2015).
15. Passaro, D. et al. Increased vascular permeability in the bone marrow microenvironment contributes to disease progression and drug response in acute myeloid leukemia. *Cancer Cell* **32**, 324 (2017).
16. Kumar, B. et al. Exosome-driven lipolysis and bone marrow niche remodeling support leukemia expansion. *Haematologica* **106**, 1484 (2021).
17. Duarte, D. et al. Inhibition of endosteal vascular niche remodeling rescues hematopoietic stem cell loss in AML. *Cell Stem Cell* **22**, 64–77.e6 (2018).
18. Berrazouane, S. et al. Beta1 integrin blockade overcomes doxorubicin resistance in human T-cell acute lymphoblastic leukemia. *Cell Death Dis.* **10**, 1–13 (2019).
19. Konopleva, M. et al. Stromal cells prevent apoptosis of AML cells by up-regulation of anti-apoptotic proteins. *Leukemia* **16**, 1713–1724 (2002).
20. Scharff, B. F. S. S., Modvig, S., Marquart, H. V. & Christensen, C. Integrin-mediated adhesion and chemoresistance of acute lymphoblastic leukemia cells residing in the bone marrow or the central nervous system. *Front Oncol.* **10**, 775 (2020).
21. Zeng, Z. et al. Inhibition of CXCR4 with the novel RCP168 peptide overcomes stroma-mediated chemoresistance in chronic and acute leukemias. *Mol. Cancer Ther.* **5**, 3113–3121 (2006).
22. Barthel, S. R., Gavino, J. D., Descheny, L. & Dimitroff, C. J. Targeting selectins and selectin ligands in inflammation and cancer. *Expert Opinion on Therapeutic Targets* **11**, 1473–1491 (2007).
23. Erbani, J., Tay, J., Barbier, V., Levesque, J. P. & Winkler, I. G. Acute Myeloid Leukemia Chemo-Resistance Is Mediated by E-selectin Receptor CD162 in Bone Marrow Niches. *Front Cell Dev Biol*. **8**, 668 (2020).
24. Barbier, V. et al. Endothelial E-selectin inhibition improves acute myeloid leukaemia therapy by disrupting vascular niche-mediated chemoresistance. *Nat. Commun.* **11**, 1–15 (2020).
25. DeAngelo, D. J. et al. Phase 1/2 study of uproleselan added to chemotherapy in patients with relapsed or refractory acute myeloid leukemia. *Blood* **139**, 1135–1146 (2022).
26. DeAngelo, D. J. et al. High E-Selectin Ligand Expression Contributes to Chemotherapy-Resistance in Poor Risk Relapsed and Refractory (R/R) Acute Myeloid Leukemia (AML) Patients and Can be Overcome with the Addition of Uproleselan. *Blood* **134**, 2690 (2019).
27. DeAngelo, D. J. et al. A phase III trial to evaluate the efficacy of uproleselan (GMI-1271) with chemotherapy in patients with relapsed/

refractory acute myeloid leukemia. *J. Clin. Oncol.* **37**, https://doi.org/10.1200/JCO.2019.37.15_suppl.TPS7066 (2019).
28. Sison, E. A. R., McIntyre, E., Magoon, D. & Brown, P. Dynamic chemotherapy-induced upregulation of CXCR4 expression: A mechanism of therapeutic resistance in pediatric AML. *Mol. Cancer Res.* **11**, 1004–1116 (2013).
29. Gruszka, A. M., Valli, D., Restelli, C. & Alcalay, M. Adhesion deregulation in acute myeloid Leukaemia. *Cells* **8**, 66 (2019).
30. Meads, M. B., Gatenby, R. A. & Dalton, W. S. Environment-mediated drug resistance: A major contributor to minimal residual disease. *Nature Reviews Cancer* **9**, 665–674 (2009).
31. Jacoby, E., Chien, C. D. & Fry, T. J. Murine Models of Acute Leukemia: Important Tools in Current Pediatric Leukemia Research. *Front. Oncol.* **4**, 95 (2014).
32. Almosailleakh, M. & Schwaller, J. Murine Models of Acute Myeloid Leukaemia. *Int. J. Mol. Sci.* **20**, 453 (2019).
33. Fiedler, E. R. C., Bhutkar, A., Lawler, E., Besada, R. & Hemann, M. T. In vivo RNAi screening identifies Pafah1b3 as a target for combination therapy with TKIs in BCR-ABL1+ BCP-ALL. *Blood Adv.* **2**, 1229–1242 (2018).
34. Wang, Y. et al. ALOX5 exhibits anti-tumor and drug-sensitizing effects in MLL-rearranged leukemia. *Sci. Rep.* **7**, 1853 (2017).
35. Meyer, C. et al. The MLL recombinome of acute leukemias in 2013. *Leukemia* **27**, 2165–2176 (2013).
36. Roumiantsev, S., De Aos, I. E., Varticovski, L., Maria, R. L. & Van Etten, R. A. The Src homology 2 domain of Bcr/Abl is required for efficient induction of chronic myeloid leukemia-like disease in mice but not for lymphoid leukemogenesis or activation of phosphatidylinositol 3-kinase. *Blood* **97**, 4–13 (2001).
37. Galbraith, P. R. Studies on the longevity, sequestration and release of the leukocytes in chronic myelogenous leukemia. *Can. Med Assoc. J.* **95**, 511–521 (1966).
38. Zhang, B. et al. Treatment-induced arteriolar revascularization and miR-126 enhancement in bone marrow niche protect leukemic stem cells in AML. *J. Hematol. Oncol.* **14**, 122 (2021).
39. Jethava, Y. S. et al. Conditioning regimens for allogeneic hematopoietic stem cell transplants in acute myeloid leukemia. *Bone. Marrow. Transplant.* **52**, 1504–1511 (2017).
40. Reshef, R. & Porter, D. L. Reduced-intensity conditioned allogeneic SCT in adults with AML. *Bone. Marrow. Transplant.* **50**, 759–769 (2015).
41. Ales, E. & Sackstein, R. The biology of E-selectin ligands in leukemogenesis. *Adv. Cancer Res* **157**, 229–250 (2023).
42. Chase, S. D., Magnani, J. L. & Simon, S. I. E-selectin ligands as mechanosensitive receptors on neutrophils in health and disease. *Ann. Biomed. Eng.* **40**, 849 (2012).
43. Shaw Bagnall, J. et al. Deformability-based cell selection with downstream immunofluorescence analysis. *Integr. Biol. (U. Kingd.)* **8**, 654–664 (2016).
44. Burg, T. P. et al. Weighing of biomolecules, single cells and single nanoparticles in fluid. *Nat.* **446**, 1066–1069 (2007).
45. Olcum, S., Cermak, N., Wasserman, S. C. & Manalis, S. R. High-speed multiple-mode mass-sensing resolves dynamic nanoscale mass distributions. *Nat. Commun.* **6**, 1–8 (2015).
46. Stevens, M. M. et al. Drug sensitivity of single cancer cells is predicted by changes in mass accumulation rate. *Nat. Biotechnol.* **34**, 1161–1167 (2016).
47. Hennigs, J. K., Matuszcak, C., Trepel, M. & Körbelin, J. Vascular Endothelial Cells: Heterogeneity and Targeting Approaches. *Cells* **10**, 2712 (2021).
48. Inoue, S. & Osmond, D. G. Basement membrane of mouse bone marrow sinusoids shows distinctive structure and proteoglycan composition: A high resolution ultrastructural study. *Anat. Rec.* **264**, 294–304 (2001).
49. Kulkarni, R. & Kale, V. Physiological Cues Involved in the Regulation of Adhesion Mechanisms in Hematopoietic Stem Cell Fate Decision. *Front. Cell. Dev. Biol.* **8**, 611 (2020).
50. Moore, M. A. S. Waking up HSCs: A new role for E-selectin. *Nat. Med.* **18**, 1613–1614 (2012).
51. Hassanshahi, M., Hassanshahi, A., Khabbazi, S., Su, Y. W. & Xian, C. J. Bone marrow sinusoidal endothelium as a facilitator/regulator of cell egress from the bone marrow. *Crit. Rev. Oncol. Hematol.* **137**, 43–56 (2019).
52. Mosteo, L. et al. The Dynamic Interface Between the Bone Marrow Vascular Niche and Hematopoietic Stem Cells in Myeloid Malignancy. *Front. Cell. Dev. Biol.* **9**, 635189 (2021).

Acknowledgements

We thank the Koch Institute's Robert A. Swanson (1969) Biotechnology Center for technical support, specifically the Flow Cytometry Core Facility, the Hope Babette Tang (1983) Histology Facility, and the Microscopy Core Facility. We thank the MIT Division of Comparative Medicine for support and guidance of animal experiments. This work was supported in part by the Virginia and D.K. Ludwig Fund for Cancer Research, the MIT Center for Cancer Precision Medicine and Stand Up to Cancer (SU2C) Convergence Program 3.1416. D.M.W. was supported by NCI R35 CA239158 and NCI P01 CA248384.

Author contributions

A.B.M, D.M.W., M.T.H. and S.R.M. conceptualized the study. A.B.M., A.L., F.H.R., D.G., A.A.L., D.M.W., M.T.H. and S.R.M. designed the experiments. A.B.M, A.L., F.H.R., L.L. and C.B., performed the blood exchange experiments. L.L. performed the animal surgeries. A.B.M. analyzed blood exchange data. A.B.M. and A.L. performed flow cytometry. A.B.M., A.L., S.D. and Y.Z. measured the leukemia cell biophysical properties. A.B.M., M.T.H. and S.R.M. wrote the paper with input from all the other authors.

Competing interests

The authors declare the following competing interests: A.B.M. is an employee of RA Capital Management. D.R.G. is an employee of Vor Biopharma Inc. D.M.W. is an employee of Merck and Co., owns equity in Merck and Co., Bantam, Ajax, and Travera, received consulting fees from Astra Zeneca, Secura, Novartis, and Roche/Genentech, and received research support from Daiichi Sankyo, Astra Zeneca, Verastem, Abbvie, Novartis, Abcura, and Surface Oncology. A.A.L. received research funding from Abbvie and Stemline therapeutics, and consulting fees from Cimeio Therapeutics, IDRx, Jnana Therapeutics, ProteinQure, and Qiagen, and has equity as an advisor for Medzown. S.R.M. owns equity in Travera and Affinity Biosensors. All other authors declare no competing interests.

Additional information

Supplementary information The online version contains supplementary material available at https://doi.org/10.1038/s42003-024-06181-x.

Correspondence and requests for materials should be addressed to Michael T. Hemann or Scott R. Manalis.

Peer review information *Communications Biology* thanks Stuart Rushworth, Richard Burt, and Magdalena Sznurkowska for their contribution to the peer review of this work. Primary Handling Editors: Toril Holien and Manuel Breuer.